



Genomic and biological characterization of the novel phages vB_VpaP_AL-1 and vB_VpaS_AL-2 infecting *Vibrio parahaemolyticus* associated with acute hepatopancreatic necrosis disease (AHPND)

Jean Pierre González-Gómez^a, Osvaldo López-Cuevas^a, Nohelia Castro-del Campo^a, Irvin González-López^a, Célida Isabel Martínez-Rodríguez^a, Bruno Gomez-Gil^b, Cristóbal Chaidez^{a,*}

^a Centro de Investigación en Alimentación y Desarrollo, A.C. (CIAD), Laboratorio Nacional para la Investigación en Inocuidad Alimentaria (LANIA), Carretera a Eldorado Km 5.5, Campo El Diez, Culiacán, Sinaloa 80110, Mexico

^b Centro de Investigación en Alimentación y Desarrollo, A.C. (CIAD), Unidad Mazatlán en Acuicultura y Manejo Ambiental, AP 711, Mazatlán, Sinaloa, Mexico

ARTICLE INFO

Keywords:
Bacteriophages
Phage therapy
Vibrio parahaemolyticus
AHPND

ABSTRACT

Acute hepatopancreatic necrosis disease (AHPND) is a life-threatening disease to recently stocked shrimp. This disease is mainly caused by *Vibrio parahaemolyticus* and, to date, it has not been effectively controlled. Bacteriophages are a promising method to control bacterial diseases in aquaculture and multiple phages that infect Asian strains of *V. parahaemolyticus* have been described. However, few studies have characterized the bacteriophages that infect Latin American strains. Here, two lytic *Vibrio* phages (vB_VpaP_AL-1 and vB_VpaS_AL-2) were isolated from estuary water in Sinaloa, Mexico. The host ranges were tested using ten AHPND-causing strains isolated from Mexico and phage AL-1 was able to infect two strains while AL-2 infected four. One-step growth curve showed that AL-1 produced 85 PFU/cell and AL-2 produced 68 PFU/cell in 30 and 40 min, respectively. Both phages were able to tolerate temperatures ranging from 20 to 50 °C and pH values ranging from 4 to 10. Phages AL-1 and AL-2 have double-stranded DNA genomes of 42,854 bp and 58,457 bp, respectively. In total, 53 putative ORFs associated with the phage structure, packing, host lysis, DNA metabolism, and additional functions were predicted in the AL-1 genome, while 92 ORFs associated with the same functions as the AL-1 and 1 tRNA were predicted in the AL-2 genome. The lifecycle was classified as virulent for both phages. Morphology, phylogeny, and comparative genomic analyses assigned phage AL-1 as a new member of the genus *Maculvirus* in the *Autographiviridae* family, and phage AL-2 as a new member of the *Siphoviridae* family. These findings suggest that vB_VpaP_AL-1 and vB_VpaS_AL-2 are potential biocontrol agents against AHPND-causing *V. parahaemolyticus* from Mexico.

1. Introduction

Vibrio parahaemolyticus is a gram-negative halophilic bacterium commonly associated with infections in aquatic organisms in aquaculture farms and the wild. In 2013, *V. parahaemolyticus* was described as the first etiological agent of acute hepatopancreatic necrosis disease (AHPND) (Tran et al., 2013), a highly virulent disease that affects several shrimp species. AHPND was formerly referred to as early mortality syndrome (EMS) because it causes a mortality rate close to 100% within the first 35 days of the postlarval stage due to severe atrophy of the hepatopancreas (Hong et al., 2016). The hepatopancreas atrophy is

mediated by the delta-endotoxin Pir, which causes the degeneration of the epithelial cells of the tubule, detachment of the basement membrane, and then shed in the lumen of the tubule, showing extensive intertubular hemocytic aggregation at the final stages (Han et al., 2015). Furthermore, these strains may possess additional virulence determinants such as adhesins, toxins, and type III secretion systems that cause enterotoxicity in animal models (Zhang and Orth, 2013; Zhou et al., 2014). The emergence of AHPND began in 2009 in China. Since then, the disease has spread in several countries including Vietnam, Thailand, the Philippines, Bangladesh, the United States, South Korea, and Mexico. The latter was the most affected country, experiencing a

* Corresponding author.

E-mail address: chaqui@ciad.mx (C. Chaidez).

<https://doi.org/10.1016/j.virusres.2022.198719>

Received 1 November 2021; Received in revised form 20 February 2022; Accepted 22 February 2022

Available online 24 February 2022

0168-1702/© 2022 Elsevier B.V. All rights reserved.

65% drop in shrimp production (tons) in two years. In addition, global economic losses caused by AHPND are estimated at US\$ 23.6 billion (Nunan et al., 2014; Shinn et al., 2018). The conventional approach thus far to mitigate AHPND has been the antibiotics-based treatment or chemical intervention (disinfection), both with limited success and potential side effects such as antibiotic resistance (Kumar et al., 2021). Furthermore, *V. parahaemolyticus* is part of the microbiota of estuarine and coastal environments, as well as shrimp in tropical areas (Thompson et al., 2004), and eliminating this species will affect the microbiota balance. Therefore, specific, safe, and environmentally friendly strategies are needed to control AHPND and prevent the development of antibiotic-resistant strains.

Phage therapy is recognized as one of the most successful techniques to combat infections as well as to reduce or eliminate bacteria in the food production environment (Bao et al., 2020; Gordillo Altamirano and Barr, 2019; Olson et al., 2021). In aquaculture, is a promising method for the prevention and treatment of vibriosis (Kalatzis et al., 2018), and several studies have applied it in shrimp ponds with satisfactory results (Karunasagar et al., 2007; Lomelí-Ortega and Martínez-Díaz, 2014; Martínez-Díaz and Hipólito-Morales, 2013; Vinod et al., 2006). Bacteriophages (phages) are viruses that infect bacteria with high host specificity, and they reproduce within bacteria and proliferate exponentially (Angulo et al., 2018; Kalatzis et al., 2018; Madhusudana Rao and Lalitha, 2015). To date, only a few attempts have been made to control AHPND in shrimp using bacteriophages, with most research focused on Asian strains of AHPND-causing *V. parahaemolyticus*. Kim et al. (2012) identified and sequenced the genome of the phage pVp-1 from the *Siphoviridae* family and Jun et al. (2016) evaluated its potential to infect AHPND-causing strains indicated that it showed a wide host range against both Asian and Mexican strains; however, no information is available on its biological characterization. Makarov et al. (2019) biologically characterized and performed a phage therapy evaluation of phages T2A2 and VH5e, which present a podovirus morphology and infect several Mexican AHPND-causing strains; however, the characteristics of its genome remain unknown. The genomic characterization of phages is crucial not only for determining whether they are safe to use but also to generate a taxonomic classification (Turner et al., 2021). Phage libraries must be increased and fully characterized to cover all AHPND-causing strain lineages to formulate phage cocktails that are effective and safe to prevent and treat this disease.

In the present study, phages vB_VpaP_AL-1 and vB_VpaS_AL-2, which present lytic activity against Mexican AHPND-causing *V. parahaemolyticus* strains, were isolated from estuarine water. The lack of virulence, antibiotic resistance, or lysogenic genes was evaluated by whole genome sequencing, and their resistance to environmental stresses and performance in the one-step growth curve were characterized to assess their suitability for phage therapy.

2. Materials and methods

2.1. Bacterial strains and growth condition

In total, 10 previously reported AHPND-causing *V. parahaemolyticus* strains isolated in Mexico (Gomez-Gil et al., 2014; González-Gómez et al., 2020) were used for bacteriophage isolation and host range

evaluation (Table 1). All strains were cultured in 5 mL of tryptic soy broth (TSB; Oxoid Ltd, Hants, UK) supplemented with 2.5% NaCl (Jalmeq, Nuevo Leon, Mexico) and incubated at 37 °C for 18–24 h. The genomes of these strains are already available in GenBank under the BioProject PRJNA604195.

2.2. Phage isolation

Seawater and estuary water samples were collected from different locations in the coastal region of Altata, Sinaloa, Mexico, and processed by the enrichment method described by Mateus et al. (2014), with some modifications. Briefly, 200 mL of water was added to 200 mL of TSB at double concentration and 1 mL of each overnight bacterial culture and then incubated at 30 °C for 18 h at 80 rpm. After incubation, the enriched samples were centrifuged at 10,000 x g for 10 min (Megafuge 16R, Thermo Fisher Scientific Inc., Waltham, Massachusetts, USA), and the supernatants were collected and filtered through a 0.22 µm pore membrane (Pall Corp., NY, USA). The filtrates were collected and used to detect the presence of lytic phages against pVA1-harboring *V. parahaemolyticus* strains by a spot test. The filtrates that showed the presence of bacteriophages were serially diluted and 100 µL of diluted supernatant was mixed with 1000 µL of an overnight culture of host bacteria in 3 mL of soft agar (TSB with 0.4% agar), poured on tryptic soy agar (TSA) plates (Oxoid Ltd, Hants, UK), and incubated at 37 °C for 18 h. Bacteriophage plaques were selected based on size and clarity and transferred to microtubes containing 1 mL of nanopure water. This procedure was repeated at least three times to ensure that the isolated phages were descendants of a single virion.

2.3. Host range

The host range of phages vB_VpaP_AL-1 and vB_VpaS_AL-2 was determined using both the spot test and the efficiency of plating (EOP) as described by Kutter (2009). Briefly, 1 mL of bacterial culture and 3 mL of soft agar were mixed and poured on a TSA plate. After solidification, 10 µL of the phage suspension was spotted onto the soft agar surface, allowed to dry at room temperature, and incubated at 37 °C for 18 h. The results were classified based on the clarity of the spot and divided into three categories: complete lysis, incomplete lysis, and no lysis. The EOP was determined for the strains with complete lysis in the spot test by the double-layer agar method, and the EOP values were calculated by dividing the average plaque-forming units (PFU) on the evaluated strain by the average PFU on the best host.

2.4. One-step growth curve

The one-step growth curves were done according to Kropinski (2018), with minor modifications. Briefly, 5 mL of the host strain culture (10^8 CFU/mL) was harvested by centrifugation (8000 x g, 5 min), resuspended in 4.5 mL of SM buffer and mixed with 0.5 mL of phage stock (10^8 PFU/mL) to obtain a multiplicity of infection (MOI) of 0.1. Phages were allowed to adsorb for 15 min at 37 °C, and then the mixture was centrifuged at 12,000 x g for 2 min. The supernatant with unabsorbed phages was discarded and the pellet was resuspended in 10 mL of TSB+2.5% NaCl. Two samples were collected (0 min), and 2-3 drops of

Table 1

Host range of vB_VpaP_AL-1 and vB_VpaS_AL-2 against AHPND-related *V. parahaemolyticus* strains.

Phage strain	Source	Host range (EOP) ^a										Plaque diameter ^b
		M0605	M0607	M0802	M0803	M0904	M0905	M2401	M2411	M2413	M2415	
AL-1	Estuary water	-	-	-	-	-	-	-	-	++ (1.00)	++ (0.95)	1 mm
AL-2	Estuary water	-	-	++ (0.79)	++ (0.83)	++ (1.00)	++ (0.92)	-	-	-	-	3 mm

^a Host range results were recorded as follows: complete lysis: ++, incomplete lysis: +, and no lysis: -.

^b Plaque diameter obtained from the double agar technique against their respective host.

chloroform were added to one sample. The mixture was incubated at 37 °C with shaking (200 rpm), and samples were collected every 10 min over a period of 80 min and titered using the soft agar overlay technique. The burst size was calculated as the ratio of the final count of liberated phage particles to the initial count of infected bacterial cells (phage titer at 0 min – phage titer at 0 min with chloroform).

2.5. Resistance to environmental stresses

To determine the stability of the phages, heat and pH tests were conducted following a previously described protocol (Cao et al., 2021). Five hundred microliters of phage suspension (10^8 PFU/mL) was incubated at different temperatures (20, 30, 40, 50, 60, and 70 °C) in a thermoblock for 1 h. For the determination of pH stability, 100 µL of phage stock was mixed with 900 µL of SM buffer with different pH values (pH 2, 3, 4, 5, 6, 7, 8, 9, 10, 11, and 12), followed by incubation at 37 °C for 1 h. The phage titer was determined by the soft agar overlay technique using the respective host.

2.6. DNA extraction and genome sequencing

Phage genomic DNA was extracted using the phenol-chloroform method (Sambrook and Russell, 2006). Briefly, 1 mL of phage suspension was transferred to a 1.5 mL microtube and treated with 10 µL of DNase I/RNase A (10 mg/mL) at 37 °C for 30 min, followed by treatment with 50 µL SDS (10%), 40 µL EDTA (0.5 M), and 2.5 µL proteinase K (20 mg/mL) and incubation at 56 °C for 2 h. An equal volume of phenol was added, mixed, and centrifuged at 3,500 x g for 10 min. The aqueous layer was transferred and mixed with an equal volume of phenol-chloroform (1:1) and centrifuged twice at 3,500 x g for 10 min. The aqueous layer was collected and mixed with an equal volume of isopropanol and stored at -20 °C overnight. The mixture was centrifuged at 15,000 x g for 30 min, and the DNA pellet was washed with ice-cold 75% ethanol three times. Finally, the DNA pellet was air-dried, resuspended in 100 µL of nuclease-free water, and stored at -20 °C.

The DNA libraries were prepared using the Nextera XT Library Preparation Kit (Illumina, San Diego, CA, USA) according to the manufacturer's instructions. The libraries were quantified using a Qubit 2.0 fluorometer (Thermo Fisher Scientific, Waltham, MA, USA) and genome sequencing was performed with the Illumina MiniSeq platform (2 × 150 bp paired-end protocol, 300 cycles). Raw reads were trimmed by fastp v0.22.0 (Chen et al., 2018) and *de-novo* assembled using SPAdes v3.15.3 (Bankevich et al., 2012), resulting in a single contig with >500X coverage for each phage genome.

2.7. Genome annotations, comparative genomics, and phylogenetic analyses

The open reading frames (ORFs) were identified by PHANOTATE v1.5.0 (McNair et al., 2019) and manually curated using Geneious v9.1.8. The ORF functions were annotated using Geneious v9.1.8 and the protein basic local alignment search tool (blastp) of the NCBI server (<https://blast.ncbi.nlm.nih.gov/Blast.cgi>) based on a search of the nonredundant protein sequence database, with a score of > 50 and an e-value of $<1.0 \times 10^{-3}$. The presence of tRNA was determined using tRNAscan-SE (Lowe and Chan, 2016) and ARAGORN (Laslett and Canback, 2004). The virulence signatures were screened using Victors (Sayers et al., 2019) and VFDB (Chen et al., 2005), and signatures of antibiotic resistance were screened using CARD (McArthur et al., 2013) and NDARO (<http://www.ncbi.nlm.nih.gov/pathogens/antimicrobial-resistance/>). Circular maps of the annotated genomes were generated using DNAPlotter v18.1.0 (Carver et al., 2009). The AI-driven software platform PhageAI v0.10.0 was used to classify the phage life-style (Tyncecki et al., 2020). For the phylogenetic analysis, a blastp search was performed for the maturase B protein for phage vB_VpaP_AL-1 and terminase large subunit protein for phage

vB_VpaS_AL-2, and the most closely related sequences of these proteins and the complete genomes of the phages were collected (Table S1). Protein sequences were aligned using ClustalW (Thompson et al., 1994) with default parameters in MEGA X (Kumar et al., 2018), and the trees were constructed using the neighbor-joining method with 1000 bootstrap replications. Complete phage genomes were assessed using the VICTOR web tool to determine the phylogenetic relationships (Meier-Kolthoff and Goker, 2017), and pairwise comparisons of the nucleotide sequences were conducted using the Genome-BLAST Distance Phylogeny (GBDP) method under the settings recommended for prokaryotic viruses. Finally, the complete genomes were used to calculate inter-genomic similarities among viral genomes through the VIRIDIC web tool (Moraru et al., 2020) with blastn default settings, and the comparison between phages and their respective closely related genomes was visualized using EasyFig v2.2.2 (Sullivan et al., 2011).

2.8. Statistical analysis

All experiments were performed in triplicate, the results are expressed as the mean ± standard deviation (SD), and the data were evaluated based on analysis of variance (ANOVA) and then, a least significant difference (LSD) test in Statgraphics Centurion XV software v15.2.06 (Statpoint Technologies, Inc., Warrenton, VA, USA).

3. Results and discussion

3.1. Isolation and general features of bacteriophages

Fifteen seawater and estuary water samples were collected and tested for the presence of phages with lytic activity against ten Mexican AHPND-causing *V. parahaemolyticus* strains. Two phages were purified based on their plaque clarity using the soft agar overlay technique and designated vB_VpaP_AL-1 and vB_VpaS_AL-2 according to the Bacterial and Archaeal Viruses Subcommittee (BAVS) of the International Committee on Taxonomy of Virus (ICTV) recommendation (Adriaenssens and Brister, 2017). Both phages formed clear plaques (approximately 1 and 3 mm in diameter) on the double-layered agar test as shown in Fig. 1. Other studies in phages that infect *V. parahaemolyticus* have reported clear plaque morphologies with diameters of 1 to 3 mm in diameter (Cao et al., 2021; Ding et al., 2020). Bacteriophages can be isolated from any environment where their host is found; however, some factors affect the rate of phage recovery in these samples, such as the sample volume, enrichment type, and incubation conditions (Alagappan et al., 2016; Makarov et al., 2019; Mateus et al., 2014; Yang et al., 2020).

3.2. Host range analysis

The results of the spot test showed that phage AL-1 lysed two AHPND-causing *V. parahaemolyticus* strains and phage AL-2 lysed four strains, which exhibited a narrow host range (Table 1). However, the

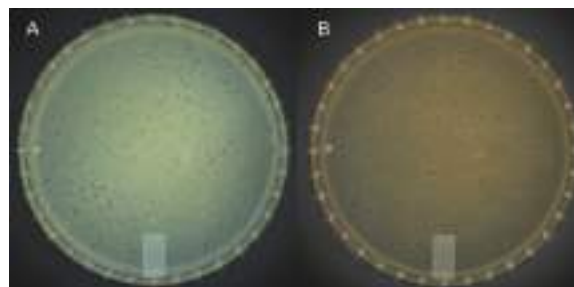


Fig. 1. Morphology of plaques formed on a double-layered agar plate by AL-1 (A) and AL-2 (B).

specific lytic activity corresponded to the subclades identified by a phylogenomic analysis of the strains in our previous work (González-Gómez et al., 2020), suggesting a possible lytic effect against the Mexican strains closely related to these subclades isolated by other research groups. Since all 10 *V. parahaemolyticus* strains were used for sample enrichment, the plating efficiency test was used to determine the most efficient host for each phage. The results showed that phage AL-1 produces a higher titer on strain M2413 and phage AL-2 produces a higher titer on strain M0904; therefore, these strains were designated as their respective hosts. The other phage-sensitive strains showed EOP values between 0.79 and 0.95 (Table 1). According to this approach, a narrow host range may be most desirable for phage therapy in marine environments because *Vibrio* is a natural inhabitant of marine environments and part of the normal microbiota of shrimp (Thompson et al., 2004). Therefore, a phage with a broad host range against *Vibrio* strains can disturb the normal microbiota, which could affect organism fitness (Pérez-Sánchez et al., 2018). However, the highly specific host range could also be a drawback that severely restricts its applicability, thus the characterization of the mechanisms and receptors involved in the adsorption of these phages is particularly important (Ge et al., 2020).

3.3. One-step growth curve

The one-step growth curve revealed latent periods of 10 min for both phages and rise periods of 30 min for phage AL-1, and 40 min for phage AL-2. Interestingly, two curves were observed in phage AL-1 due to its short latency and growth periods. Burst size was determined to be 85 PFU/cell for phage AL-1 (Fig. 2B) and 68 PFU/cell for phage AL-2 (Fig. 2D). The burst size and latency period represent very valuable data since one of the advantages of phage therapy is that lytic phages continue to amplify at the site of infection until cells are no longer available to infect (Madhusudana Rao and Lalitha, 2015); thus, the one-step growth curve is a fundamental test for phage characterization.

3.4. Resistance to environmental stresses

We exposed phages AL-1 and AL-2 to different temperatures and pH ranges for one hour to investigate their stability under environmental stresses. As shown in Fig. 2A, the titers of both phages were stable at approximately 8 Log₁₀ PFU/mL after exposure to temperatures between 20 and 40 °C. After exposure to 50 °C, both phage titers significantly decreased ($p < 0.05$) to ~x223C7.4 Log₁₀ PFU/mL, while after exposure to 60 °C titers of both phages significantly decreased to ~x223C4 Log₁₀ PFU/mL. Exposure to 70 °C completely inactivated both phages. Both phages remained highly infective at pH values ranging from 4 to 9 (Fig. 2C). After exposure to pH 3, 10, and 11, both phages showed significant titer reduction ($p < 0.05$), although the reduction at pH 10 was ~x223C1 Log₁₀ PFU/mL in both phages. AL-1 and AL-2 were inactivated after exposure to pH 2. The results obtained in the environmental stress tolerance tests suggest that both phages can be applied in harsh environments. In shrimp ponds, the temperature fluctuates between 23 and 33 °C (Rahman et al., 2007) and the pH fluctuates between 6 and 10 (Yu et al., 2020), and the phages can remain stable in these ranges.

3.5. General features of genomes analysis

Both phages have a linear double-stranded DNA genome (Fig. 3). The genome of phage AL-1 was 42,854 bp long and had an average GC content of 49.1%, while AL-2 was 58,457 bp and had an average GC content of 46.4%. The AL-1 genome contained 53 putative ORFs located in the forward strand, with an average length of 779 bp and sizes ranging from 93 to 3855 nucleotides. Otherwise, 92 putative ORFs were predicted in the genome of phage AL-2, which are located in forward (36) and reverse (56) strands, with an average length of 587 bp and sizes ranging from 99 to 2,400 bp. Of the 53 putative ORFs in the AL-1 genome, 22 were assigned to hypothetical proteins and 14, 8, 2, 4, and 3 were predicted to encode proteins associated with DNA

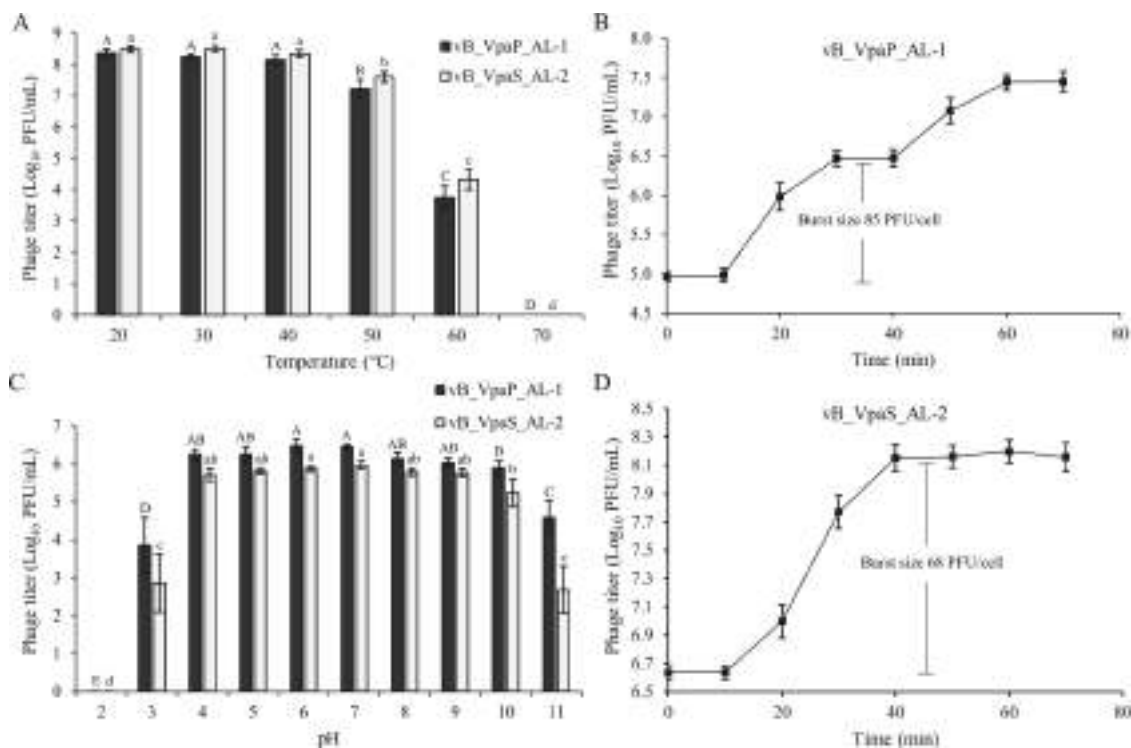


Fig. 2. Biological characterization of vB_VpaP_AL-1 and vB_VpaS_AL-2. (A) Stability of phages AL-1 and AL-2 at various temperatures for 1 h. (B) One-step growth curve of phage AL-1. (C) Stability of phages AL-1 and AL-2 at various pH values for 1 h. (D) One-step growth curve of phage AL-2. Different uppercase letters on stability assays indicate a significant difference ($p < 0.05$) between AL-1 treatments and lower case letters indicate a significant difference in AL-2 treatments. Values are the means of three tests \pm standard deviation.

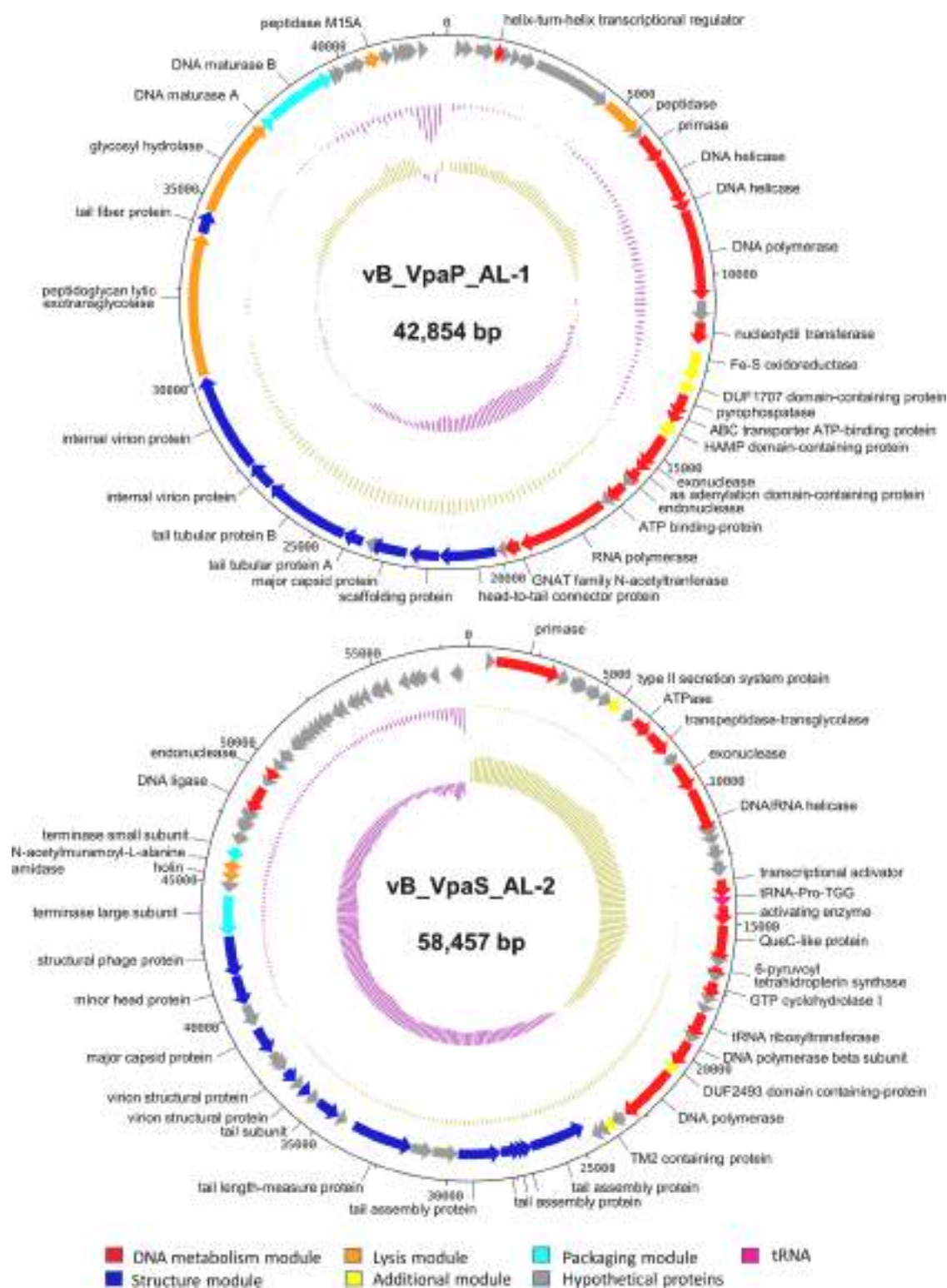


Fig. 3. Genome maps of phages vB_VpaP_AL-1 and vB_VpaS_AL-2. The two innermost circles represent GC skew and GC content, respectively. Arrows indicate annotated ORFs, with either rightward or leftward direction, and color-coded by their putative function.

metabolism, structural proteins, packaging, lysis functions, and additional modules. In addition, only 24 putative ORFs in the AL-2 genome were predicted to encode proteins associated with DNA metabolism (15), structure functions (12), packaging (2), lysis functions (2), and additional modules (3); thus, the function of most of its genes remains uncharacterized.

The genome of phage AL-1 has several features that have been

described in closely related phage genomes. Hu et al. (2020) showed that in addition to tail fiber binding to LPS, tubular tail proteins A and B bind to transmembrane proteins, which mediates phage adsorption and bacterial lysis. In addition, Kp32 phage tubular tail protein A also shows enzymatic activity to hydrolyze polysaccharides (Brzozowska et al., 2017), suggesting antibiofilm activity. Furthermore, phage AL-1 can be efficiently transcribed in the middle and late stages of its infection since

it possesses a large subunit RNA polymerase (Turner et al., 2019; Yang et al., 2014). Lim et al. (2020) evaluated the lytic activity of glycosyl hydrolase and zinc peptidase present in phage KF2, and the peptidase showed more significant lytic activity with a broader spectrum compared to the KF2 host range.

Compared with AL-1, none of the phage AL-2 genomic features have been described in closely related genomes. Most of the protein families present in the AL-2 phage genome have been studied in other siphophages, however, the T5 phage is widely used as a model phage (Nobrega et al., 2018) and was recently reclassified in the new family *Demereviridae* (Kropinski et al., 2019). Only four phages with >70% similarity have been described at the time of writing; therefore, additional studies on these phages genomes are required and a large number of hypothetical proteins and their functions in phage infection need to be further characterized. Furthermore, it is necessary to identify the binding sites of the phages, since it has been reported that other phages of the *Siphoviridae* family bind to the flagellum, causing the loss of this organelle in the phage-resistant strains of *Vibrio* (Li et al., 2021). In this way, phage therapy can have added value by reducing the virulence of these pathogenic strains.

Finally, one tRNA gene encoding proline was found in the AL-2 genome. Since phages have extremely compact genomes that reduce their ability to take advantage of host resources, tRNAs could compensate for compositional differences between phages and hosts and complement the translation machinery based on their genetic information to obtain higher fitness and produce stronger virulence (Bailly-Bechet et al., 2007). No antibiotic resistance, virulence, or lysogenic genes were found in either genome, and the phage lifestyle was predicted to be

virulent by PhageAI. Phage therapy could be harmful if the phage's genomic content is not properly characterized due to its ability to interact with its host's DNA; consequently, an extensive analysis of the genome of each phage involved in phage therapy must be performed to identify undesirable traits (Culot et al., 2019).

3.6. Phylogenetic and comparative genomic analysis

The taxonomic classification of bacteriophages has been in flux in recent years. Since 1998, when the ICTV recognized the unification of tailed phages within the order *Caudovirales*, the morphology of the phages was the only criterion for assigning them to the *Podoviridae*, *Myoviridae*, and *Siphoviridae* families. The development of sequencing technologies and comparative genomic analyses have called for the establishment of a better taxonomic classification with precise criteria for the demarcations between the different taxonomic ranks. At the time of writing this article, 14 families have been recognized within the order *Caudovirales*. The ICTV's Bacterial and Archaeal Viruses Subcommittee recently recommended the demarcation of families based on cohesive and monophyletic clustering using the main predicted proteome-based clustering tools. Genus demarcation is established by >70% nucleotide identity over the full genome length, and species demarcation is established by >95% nucleotide identity over their full genome length (Turner et al., 2021).

To assign a taxonomic classification to phage vB_VpaP_AL-1, two phylogenetic trees based on the maturase B protein (Figure S1A) and whole-genome (Fig. 4A) were constructed, and intergenomic similarities (Fig. 4B) were calculated between the closely related genomes reported

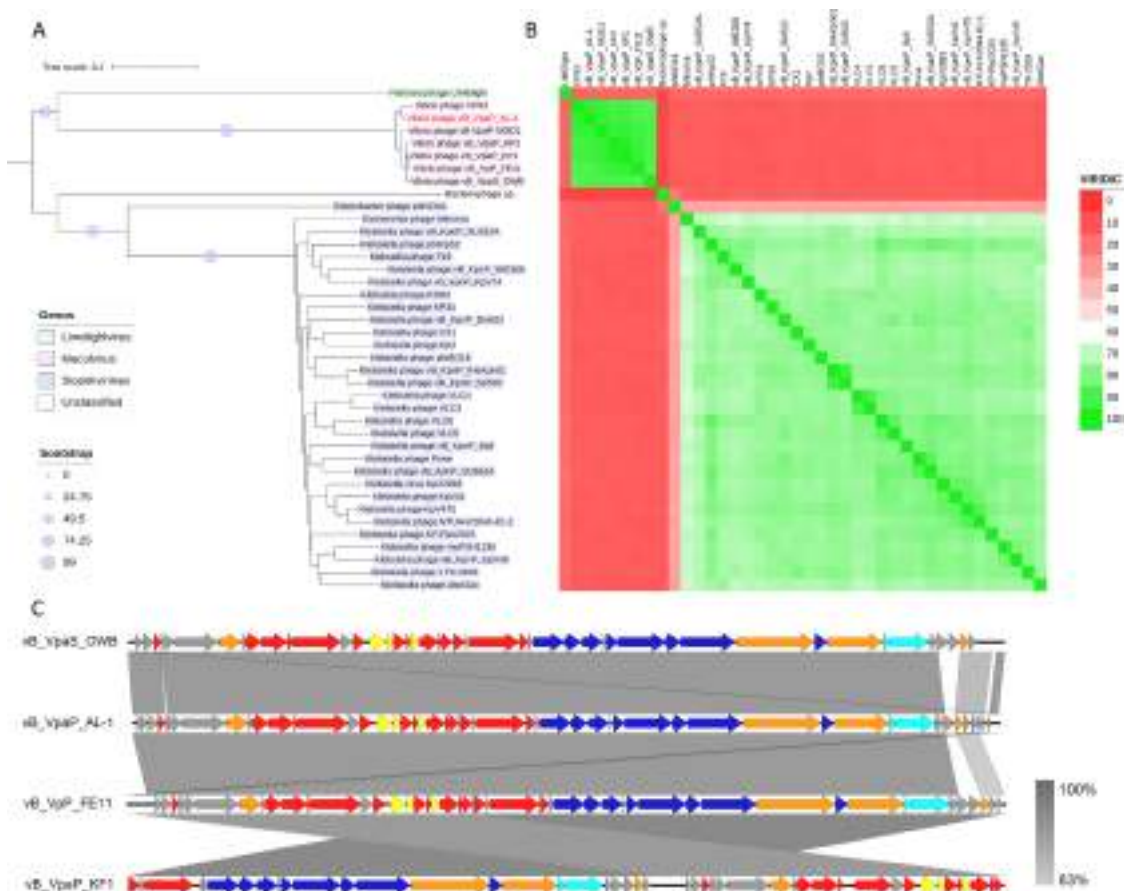


Fig. 4. Genomic and phylogenetic analysis of phage vB_VpaP_AL-1. (A) Phylogenetic tree based on Genome-BLAST Distance Phylogeny (GBDP) of vB_VpaP_AL-1 and 39 related members of the *Podoviridae* family. (B) VIRIDIC heatmap based on intergenomic similarities amongst viral genomes represented by the color scale as similarity percentage. (C) Genome comparison of phage vB_VpaP_AL-1 and closely related members of the *Maculvirus* genus. Color scales represent the percentage nucleotide identity between regions obtained through blastn and arrows represent ORFs, either rightward or leftward direction.

in GenBank. Both phylogenetic trees and intergenomic similarity heatmaps revealed that phage AL-1 is a new member of the *Maculvirus* genus within the *Autographiviridae* family. Phages VP93, MGD1, KF2, KF1, FE11, and OWB were previously assigned to this classification. Most of the phages within the genus *Maculvirus* share between 87.81 and 94.55% intergenomic similarity, although phages KF1 and KF2 share 96.52% of similarity (Table S2); therefore, they belong to the same species. The other phages included in the analysis were classified into the genera *Slopekvirinae* and *Limelightvirus*, although phage phiKDA1 appears to be misclassified in its GenBank description within the genus *Slopekvirinae* (~x223C33% intergenomic similarity among other genus members), and one phage remains unclassified. The *Autographiviridae* family consists of a podovirus with a small icosahedral head attached to a short tail, and all members encode a large single subunit RNA polymerase that is responsible for mid-transcription and late transcription. Furthermore, these viruses possess genus-specific lysis cassettes (Turner et al., 2019), as shown in Fig. 5. All four compared genomes of the *Maculvirus* phages showed a lysis module near the packaging proteins. This lysis module consists of four putative enzymes: peptidoglycan lytic exotransglycolase, glycosyl hydrolase, and two peptidases, associated with cell wall degradation through peptidoglycan cleavage, leading to the cell lysis and release of phage progeny (Grabowski et al., 2021; Lim et al., 2020; Yuan and Gao, 2016;). Furthermore, Yang et al. (2022) demonstrated that phage vB_VpP_DE17 of the genus *Maculvirus* had a certain bactericidal effect against *V. parahaemolyticus* within 6 h. Also, Lomeli-Ortega et al. (2021) demonstrated that *Maculvirus* phage vB_Vc_SrVc9 is an effective agent in preventing *Vibrio campbellii* infections in *Artemia franciscana*; however, this study was based on the information obtained from 16S rRNA sequencing. Therefore, functional metagenomics is required to thoroughly evaluate the effect of these

phages on the bacteriome and virome.

Similarly, the taxonomic classification for phage vB_VpaS_AL-2 was assigned through two phylogenetic trees based on terminase large subunit proteins (Fig. S1A), whole-genomes (Fig. 5A), and intergenomic similarities (Fig. 5B) between the closely related genomes. These analyses showed that phage AL-2 belongs to a new genus within the *Siphoviridae* family, including VspDsh_1, BA3, and CA8 phages. The phylogenetic tree based on the terminase large subunits groups the phage PH699 (Hu et al., 2021) in this same clade; nevertheless, its genome is fragmented into three scaffolds, thus excluding it from whole-genome analyses. Each phage of this new genus represents a different species due to their intergenomic similarities, which range between 79.34% and 93.55% (Table S3). The other phages included in the genomic comparisons were very distant from this new genus (<26.17% similarity) despite belonging to the *Siphoviridae* family. Turner et al. (2021) advocated the abolition of the classic families *Siphoviridae*, *Myoviridae*, and *Podoviridae* in future research on the phage's taxonomic classification since there are members within these families that do not share a significant number of orthologous genes for the phylogenetic analyses. The genome comparison showed high homology among phages AL-2, CA3, and BA8; however, the genome of phage vpDsh_1 lacks an ~x223C 12,000 bp fragment that consists mostly of hypothetical proteins and two DNA metabolism-related proteins. No differences were observed in the arrangement of functional modules among phages AL-2, CA3, and BA8, and the nonhomologous regions were putative hypothetical proteins. Only two studies have described the phages belonging to this new genus (Hu et al., 2021; Yang et al., 2020); therefore, it is necessary to elaborate and present the proposed new genus to the ICTV, and new members of the genus should be further isolated and their genomes should be reported. Finally, other

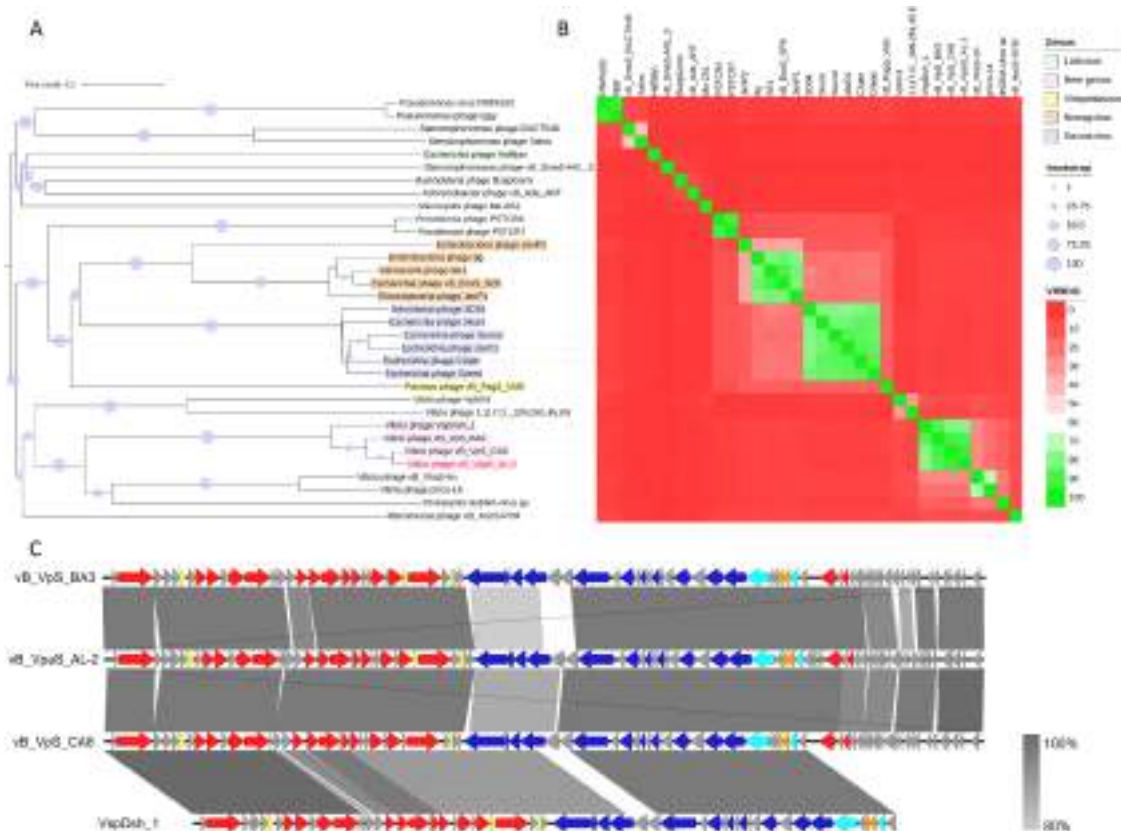


Fig. 5. Genomic and phylogenetic analysis of phage vB_VpaS_AL-2. (A) Phylogenetic tree based on Genome-BLAST Distance Phylogeny (GBDP) of vB_VpaP_AL-1 and 33 related members of the *Siphoviridae* family. (B) VIRIDIC heatmap based on intergenomic similarities amongst viral genomes represented by the color scale as similarity percentage. (C) Genome comparison of phage vB_VpaP_AL-1 and closely related members of its genus. Color scale represents the percentage nucleotide identity between regions obtained through blastn and arrows represent ORFs, either rightward or leftward direction.

siphoviruses have shown a protective effect in shrimp infected with AHPND-causing *V. parahaemolyticus* (Jun et al., 2018); however, phage therapy must be evaluated to monitor microbiota changes and the possible associated side effects in the shrimp fitness.

4. Conclusion

In conclusion, we isolated and characterized novel lytic phages vB_VpaP_AL-1 and vB_VpaS_AL-2, which belong to *Autographiviridae* and *Siphoviridae*, respectively. Both phages were able to infect at least two AHPND-causing *V. parahaemolyticus* strains isolated in Mexico and showed adequate stability under environmental stresses. Furthermore, phage AL-1 produced 85 virions per infected cell in 30 min and phage AL-2 produced 68 virions per cell in 40 min, indicating their ability to lyse bacteria quickly and effectively. The phage genomes were sequenced, assembled, and annotated, and they showed putative ORFs and tRNAs classified into various modules; nevertheless, genes associated with virulence, lysogeny, or antibiotic resistance were not found. These findings provide evidence that the phages vB_VpaP_AL-1 and vB_VpaS_AL-2 have the potential as safe and suitable biological control agents for AHPND caused by *V. parahaemolyticus*. However, it is necessary to test its effectiveness in a real natural environment and its effect against other bacteria. Therefore, in our future studies, phage therapy will be applied to shrimp ponds exposed to AHPND-causing strains to assess their effect on shrimp survival and changes in pond microbiota composition to obtain a comprehensive perspective of the outcome of phage therapy applied to a complex aquatic environment.

Data availability

The complete genome sequences of phages vB_VpaP_AL-1 and vB_VpaS_AL-2 have been deposited in the GenBank database under the accession numbers OK349506 and OK349507, respectively.

CRediT authorship contribution statement

Jean Pierre González-Gómez: Conceptualization, Formal analysis, Methodology, Writing – original draft. **Oswaldo López-Cuevas:** Conceptualization, Validation, Writing – review & editing. **Nohelia Castro-del Campo:** Formal analysis, Methodology, Writing – review & editing. **Irvin González-López:** Conceptualization, Validation, Writing – review & editing. **Célida Isabel Martínez-Rodríguez:** Conceptualization, Validation, Writing – review & editing. **Bruno Gomez-Gil:** Conceptualization, Funding acquisition, Validation, Writing – review & editing. **Cristóbal Chaidez:** Conceptualization, Funding acquisition, Validation, Writing – review & editing.

Declaration of Competing Interest

The authors declare that they have no known competing financial interests or personal relationships that could have appeared to influence the work reported in this paper.

Acknowledgments

We thank the CONACyT for the scholarship granted to Jean Pierre González-Gómez. The authors would like to thank Julissa Enciso-Ibarra, Alma Karen Orozco-Ochoa, Juan Manuel Serrano-Hernández, Annet Soto, and Berenice González-Torres for the technical support.

Funding

This work was supported by the Consejo Nacional de Ciencia y Tecnología (CONACyT) of Mexico through a scholarship granted to Jean Pierre González-Gómez [No. 818472].

Supplementary materials

Supplementary material associated with this article can be found, in the online version, at doi:10.1016/j.virusres.2022.198719.

References

- Adriaenssens, E., Brister, J.R., 2017. How to name and classify your phage: an informal guide. *Viruses* 9 (4), 70. <https://doi.org/10.3390/v9040070>.
- Alagappan, K., Karuppiah, V., Deivasigamani, B., 2016. Protective effect of phages on experimental *V. parahaemolyticus* infection and immune response in shrimp (Fabricius, 1798). *Aquaculture* 453, 86–92. <https://doi.org/10.1016/j.aquaculture.2015.11.037>.
- Angulo, C., Loera-Muro, A., Trujillo, E., Luna-González, A., 2018. Control of AHPND by phages: a promising biotechnological approach. *Rev. Aquac.* 1–16. <https://doi.org/10.1111/raq.12275>.
- Bailey-Bechet, M., Vergassola, M., Rocha, E., 2007. Causes for the intriguing presence of tRNAs in phages. *Genome Res.* 17 (10), 1486–1495. <https://doi.org/10.1101/gr.6649807>.
- Bankевич, A., Nurk, S., Antipov, D., Gurevich, A.A., Dvorkin, M., Kulikov, A.S., Lesin, V. M., Nikolenko, S.I., Pham, S., Pribelski, A.D., Pyshkin, A.V., Sirotkin, A.V., Vyahhi, N., Tesler, G., Alekseyev, M.A., Pevzner, P.A., 2012. SPAdes: a new genome assembly algorithm and its applications to single-cell sequencing. *J. Comput. Biol.* 19 (5), 455–477. <https://doi.org/10.1089/cmb.2012.0021>.
- Bao, H., Zhou, Y., Shahin, K., Zhang, H., Cao, F., Pang, M., Zhang, X., Zhu, S., Olaniran, A., Schmidt, S., Wang, R., 2020. The complete genome of lytic *Salmonella* phage vB_SenM-PA13076 and therapeutic potency in the treatment of lethal *Salmonella* enteritidis infections in mice. *Microbiol. Res.* 237, 126471. <https://doi.org/10.1016/j.micres.2020.126471>.
- Brzozowska, E., Pyra, A., Pawlik, K., Janik, M., Gorska, S., Urbanska, N., Drulis-Kawa, Z., Gamin, A., 2017. Hydrolytic activity determination of tail tubular protein A of *Klebsiella pneumoniae* bacteriophages towards saccharide substrates. *Sci. Rep.* 7 (1), 18048. <https://doi.org/10.1038/s41598-017-18096-1>.
- Cao, Y., Zhang, Y., Lan, W., Sun, X., 2021. Characterization of vB_VpaP_MGD2, a newly isolated bacteriophage with biocontrol potential against multidrug-resistant *Vibrio parahaemolyticus*. *Arch. Virol.* 166 (2), 413–426. <https://doi.org/10.1007/s00705-020-04887-x>.
- Carver, T., Thomson, N., Bleasby, A., Berriman, M., Parkhill, J., 2009. DNAPlotter: circular and linear interactive genome visualization. *Bioinformatics* 25 (1), 119–120. <https://doi.org/10.1093/bioinformatics/btn578>.
- Chen, L., Yang, J., Yu, J., Yao, Z., Sun, L., Shen, Y., Jin, Q., 2005. VFDB: a reference database for bacterial virulence factors. *Nucleic Acids Res.* 33, D325–D328. <https://doi.org/10.1093/nar/gki008> (Database issue).
- Chen, S., Zhou, Y., Chen, Y., Gu, J., 2018. fastp: an ultra-fast all-in-one FASTQ preprocessor. *Bioinformatics* 34 (17), i884–i890. <https://doi.org/10.1093/bioinformatics/bty560>.
- Culot, A., Grosset, N., Gautier, M., 2019. Overcoming the challenges of phage therapy for industrial aquaculture: a review. *Aquaculture* 513, 734423. <https://doi.org/10.1016/j.aquaculture.2019.734423>.
- Ding, T., Sun, H., Pan, Q., Zhao, F., Zhang, Z., Ren, H., 2020. Isolation and characterization of *Vibrio parahaemolyticus* bacteriophage vB_VpaS_PG07. *Virus Res.* 286, 198080. <https://doi.org/10.1016/j.virusres.2020.198080>.
- Ge, H., Hu, M., Zhao, G., Du, Y., Xu, N., Chen, X., Jiao, X.a., 2020. The "fighting wisdom and bravery" of tailed phage and host in the process of adsorption. *Microbiol. Res.* 230, 126344. <https://doi.org/10.1016/j.micres.2019.126344>.
- Gomez-Gil, B., Soto-Rodríguez, S., Lozano, R., Betancourt-Lozano, M., 2014. Draft genome sequence of *Vibrio parahaemolyticus* strain M0605, which causes severe mortalities of shrimps in Mexico. *Genome Announc* 2 (2). <https://doi.org/10.1128/genomeA.00055-14.e00055-00014>.
- González-Gómez, J.P., Soto-Rodríguez, S., López-Cuevas, O., Castro-Del Campo, N., Chaidez, C., Gomez-Gil, B., 2020. Phylogenomic analysis supports two possible origins for latin American strains of *Vibrio parahaemolyticus* associated with acute hepatopancreatic necrosis disease (AHPND). *Curr. Microbiol.* 77 (12), 3851–3860. <https://doi.org/10.1007/s00284-020-02214-w>.
- Gordillo Altamirano, F.L., Barr, J.J., 2019. Phage therapy in the postantibiotic era. *Clin. Microbiol. Rev.* 32 (2). <https://doi.org/10.1128/CMR.00666-18>.
- Grabowski, L., Lepek, K., Stasiłojc, M., Kosznik-Kwasnicka, K., Zdrojewska, K., Maciag-Dorszynska, M., Wegrzyn, G., Wegrzyn, A., 2021. Bacteriophage-encoded enzymes destroying bacterial cell membranes and walls, and their potential use as antimicrobial agents. *Microbiol. Res.* 248, 126746. <https://doi.org/10.1016/j.micres.2021.126746>.
- Han, J.E., Tang, K.F.J., Tran, L.H., Lightner, D.V., 2015. *Photobacterium* insect-related (Pir) toxin-like genes in a plasmid of *Vibrio parahaemolyticus*, the causative agent of acute hepatopancreatic necrosis disease (AHPND) of shrimp. *Dis. Aquat. Org.* 113 (1), 33–40. <https://doi.org/10.3354/dao02830>.
- Hong, X., Lu, L., Xu, D., 2016. Progress in research on acute hepatopancreatic necrosis disease (AHPND). *Aquac. Int.* 24 (2), 577–593. <https://doi.org/10.1007/s10499-015-9948-x>.
- Hu, M., Zhang, H., Gu, D., Ma, Y., Zhou, X., 2020. Identification of a novel bacterial receptor that binds tail tubular proteins and mediates phage infection of *Vibrio parahaemolyticus*. *Emerg. Microbes Infect.* 9 (1), 855–867. <https://doi.org/10.1080/22221751.2020.1754134>.
- Hu, Z., Chen, X., Chen, W., Li, P., Bao, C., Zhu, L., Zhang, H., Dong, C., Zhang, W., 2021. *Siphoviridae* phage PH669 capable of lysing some strains of O₃ and O₄ serotypes in

- Vibrio parahaemolyticus*. *Aquaculture* 545. <https://doi.org/10.1016/j.aquaculture.2021.737192>.
- Jun, J.W., Han, J.E., Giri, S.S., Tang, K.F.J., Zhou, X., Aranguren, L.F., Kim, H.J., Saekil, Y., Chi, C., Kim, S.G., Park, S.C., 2018. Phage application for the protection from acute hepatopancreatic necrosis disease (AHPND) in *Penaeus vannamei*. *Indian J. Microbiol.* 58 (1), 114–117. <https://doi.org/10.1007/s12088-017-0694-9>.
- Jun, J.W., Han, J.E., Tang, K.F.J., Lightner, D.V., Kim, J., Seo, S.W., Park, S.C., 2016. Potential application of bacteriophage pVp-1: agent combating *Vibrio parahaemolyticus* strains associated with acute hepatopancreatic necrosis disease (AHPND) in shrimp. *Aquaculture* 457, 100–103. <https://doi.org/10.1016/j.aquaculture.2016.02.018>.
- Kalatzis, P.G., Castillo, D., Katharios, P., Middelboe, M., 2018. Bacteriophage interactions with marine pathogenic Vibrios: implications for phage therapy. *Antibiotics* 7 (1), 15. <https://doi.org/10.3390/antibiotics7010015> (Basel).
- Karunasagar, I., Shivu, M.M., Girisha, S.K., Krohne, G., Karunasagar, I., 2007. Biocontrol of pathogens in shrimp hatcheries using bacteriophages. *Aquaculture* 268 (1–4), 288–292. <https://doi.org/10.1016/j.aquaculture.2007.04.049>.
- Kim, J.H., Jun, J.W., Choresca, C.H., Shin, S.P., Han, J.E., Park, S.C., 2012. Complete genome sequence of a novel marine siphovirus, pVp-1, infecting *Vibrio parahaemolyticus*. *J. Virol.* 86 (12), 7013–7014. <https://doi.org/10.1128/JVI.00742-12>.
- Kropinski, A.M., Clokie, M., Kropinski, A., Lavigne, R., 2018. Practical advice on the one-step growth curve. In: *Bacteriophages. Methods in Molecular Biology*, 1681. Humana Press, New York, NY. https://doi.org/10.1007/978-1-4939-7343-9_3.
- Kropinski, A.M., Adriaenssens, E.M., Sullivan, M.B., Tóth, I., Bishop-Lilly, K.A., Lueder, M.R., Bin, J.H., Barylski, J., 2019. Create one new family (*Demereviridae*) including three new subfamilies and six genera in the order *Caudovirales* 2019.099B. Phage. Canada@gmail.com. <https://icvtv.global/ICTV/proposals/2019.099B.zip>. Accessed 9 Aug 2021.
- Kumar, S., Stecher, G., Li, M., Nkay, C., Tamura, K., 2018. MEGA X: molecular evolutionary genetics analysis across computing platforms. *Mol. Biol. Evol.* 35 (6), 1547–1549. <https://doi.org/10.1093/molbev/msy096>.
- Kumar, V., Roy, S., Behera, B.K., Bossier, P., Das, B.K., 2021. Acute hepatopancreatic necrosis disease (AHPND): virulence, pathogenesis and mitigation strategies in shrimp aquaculture. *Toxins* 13 (8), 524. <https://doi.org/10.3390/toxins13080524> (Basel).
- Kutter, E., Clokie, M.R., Kropinski, A.M., 2009. Phage host range and efficiency of plating. In: *Bacteriophages. Methods in Molecular Biology*, 501. Humana Press. https://doi.org/10.1007/978-1-60327-164-6_14.
- Laslett, D., Canback, B., 2004. ARAGORN, a program to detect tRNA genes and tmRNA genes in nucleotide sequences. *Nucleic Acids Res.* 32 (1), 11–16. <https://doi.org/10.1093/nar/gkh152>.
- Li, J., Tian, F., Hu, Y., Lin, W., Liu, Y., Zhao, F., Ren, H., Pan, Q., Shi, T., Tong, Y., 2021. Characterization and genomic analysis of BUCT549, a novel bacteriophage infecting *Vibrio alginolyticus* with flagella as receptor. *Front. Microbiol.* 12, 668319. <https://doi.org/10.3389/fmicb.2021.668319>.
- Lim, J.A., Lee, N., Chun, H.S., Chang, H.J., 2020. Characterization of a novel endolysin from bacteriophage infecting *Vibrio parahaemolyticus*, vB_VpAp_KF2. *Appl. Biol. Chem.* 63 (1) <https://doi.org/10.1186/s13765-020-00523-z>.
- Lomeli-Ortega, C.O., Martínez-Díaz, S.F., 2014. Phage therapy against *Vibrio parahaemolyticus* infection in the whiteleg shrimp (*Litopenaeus vannamei*) larvae. *Aquaculture* 434, 208–211. <https://doi.org/10.1016/j.aquaculture.2014.08.018>.
- Lomeli-Ortega, C.O., Martínez-Sánchez, A.J., Barajas-Sandoval, D.R., Reyes, A.G., Magallón-Barajas, F., Veyrand-Quirós, B., Gannon, L., Harrison, C., Michniewski, S., Millard, A., Quiroz-Guzmán, E., 2021. Isolation and characterization of vibriophage vB_VcSrVc9: an effective agent in preventing *Vibrio campbellii* infections in brine shrimp nauplii (*Artemia franciscana*). *J. Appl. Microbiol.* 131 (1), 36–49. <https://doi.org/10.1111/jam.14937>.
- Lowe, T.M., Chan, P.P., 2016. tRNAscan-SE On-line: integrating search and context for analysis of transfer RNA genes. *Nucleic Acids Res.* 44 (W1), W54–W57. <https://doi.org/10.1093/nar/gkw413>.
- Madhusudana Rao, B., Lalitha, K.V., 2015. Bacteriophages for aquaculture: are they beneficial or inimical. *Aquaculture* 437, 146–154. <https://doi.org/10.1016/j.aquaculture.2014.11.039>.
- Makarov, R., Lomeli-Ortega, C.O., Zermeño-Cervantes, L.A., García-Álvarez, E., Gutiérrez-Rivera, J.N., Cardona-Félix, C.S., Martínez-Díaz, S.F., 2019. Evaluation of a cocktail of phages for the control of presumptive *Vibrio parahaemolyticus* strains associated to acute hepatopancreatic necrosis disease. *Aquac. Res.* 00, 1–10. <https://doi.org/10.1111/are.14258>.
- Martínez-Díaz, S.F., Hipólito-Morales, A., 2013. Efficacy of phage therapy to prevent mortality during the vibriosis of brine shrimp. *Aquaculture* 400–401, 120–124. <https://doi.org/10.1016/j.aquaculture.2013.03.007>.
- Mateus, L., Costa, L., Silva, Y.J., Pereira, C., Cunha, A., Almeida, A., 2014. Efficiency of phage cocktails in the inactivation of *Vibrio* in aquaculture. *Aquaculture* 424–425, 167–173. <https://doi.org/10.1016/j.aquaculture.2014.01.001>.
- McArthur, A.G., Waglechner, N., Nizam, F., Yan, A., Azad, M.A., Baylay, A.J., Bhullar, K., Canova, M.J., De Pascale, G., Ejim, L., Kalan, L., King, A.M., Koteva, K., Morar, M., Mulvey, M.R., O'Brien, J.S., Pawlowski, A.C., Piddock, L.J.V., Spanogiannopoulos, P., Sutherland, A.D., Tang, I., Taylor, P.L., Thaker, M., Wang, W., Yan, M., Yu, T., Wright, G.D., 2013. The comprehensive antibiotic resistance database. *Antimicrob. Agents Chemother.* 57 (7), 3348–3357. <https://doi.org/10.1128/AAC.00419-13>.
- McNair, K., Zhou, C., Dinsdale, E.A., Souza, B., Edwards, R.A., 2019. PHANOTATE: a novel approach to gene identification in phage genomes. *Bioinformatics* 35 (22), 4537–4542. <https://doi.org/10.1093/bioinformatics/btz265>.
- Meier-Kolthoff, J.P., Goker, M., 2017. VICTOR: genome-based phylogeny and classification of prokaryotic viruses. *Bioinformatics* 33 (21), 3396–3404. <https://doi.org/10.1093/bioinformatics/btx440>.
- Moraru, C., Varsani, A., Kropinski, A.M., 2020. VIRIDIC-a novel tool to calculate the intergenomic similarities of prokaryote-infecting viruses. *Viruses* 12 (11). <https://doi.org/10.3390/v12111268>.
- Nobrega, F.L., Vlot, M., de Jonge, P.A., Dreesens, L.L., Beaumont, H.J.E., Lavigne, R., Dutilh, B.E., Brouns, S.J.J., 2018. Targeting mechanisms of tailed bacteriophages. *Nat. Rev. Microbiol.* 16 (12), 760–773. <https://doi.org/10.1038/s41579-018-0070-8>.
- Nunan, L., Lightner, D., Pantoja, C., Gomez-Jimenez, S., 2014. Detection of acute hepatopancreatic necrosis disease (AHPND) in Mexico. *Dis. Aquat. Org.* 111 (1), 81–86. <https://doi.org/10.3354/dao02776>.
- Olson, E.G., Micciche, A.C., Rothrock, M.J.J., Yang, Y., Ricke, S.C., 2021. Application of bacteriophages to limit *Campylobacter* in poultry production. *Front. Microbiol.* 12, 458721. <https://doi.org/10.3389/fmicb.2021.458721>.
- Pérez-Sánchez, T., Mora-Sánchez, B., Balcázar, J.L., 2018. Biological approaches for disease control in aquaculture: advantages, limitations and challenges. *Trends Microbiol.* 26 (11), 896–903. <https://doi.org/10.1016/j.tim.2018.05.002>.
- Rahman, M.M., Corteel, M., Dantas-Lima, J.J., Wille, M., Alday-Sanz, V., Pensart, M.B., Sorgeloos, P., Nauwynck, H.J., 2007. Impact of daily fluctuations of optimum (27°C) and high water temperature (33°C) on *Penaeus vannamei* juveniles infected with white spot syndrome virus (WSSV). *Aquaculture* 269 (1–4), 107–113. <https://doi.org/10.1016/j.aquaculture.2007.04.056>.
- Sambrook, J., Russell, D.W., 2006. Extraction of bacteriophage lambda DNA from large-scale cultures using proteinase K and SDS. *CSH Protoc* (1). <https://doi.org/10.1101/pdb.prot3972>, 2006pdb.prot3972.
- Sayers, S., Li, L., Ong, E., Deng, S., Fu, G., Lin, Y., Yang, B., Zhang, S., Fa, Z., Zhao, B., Xiang, Z., Li, Y., Zhao, X.M., Olszewski, M.A., Chen, L., He, Y., 2019. Victors: a web-based knowledge base of virulence factors in human and animal pathogens. *Nucleic Acids Res.* 47 (D1), D693–D700. <https://doi.org/10.1093/nar/gky999>.
- Shinn, A., Pratoomyot, J., Griffiths, D., Trong, T., Vu, N., Jiravanichpaisal, P., Briggs, M., 2018. Asian shrimp production and the economic costs of disease. *Asian Fish. Sci.* 31, 29–58.
- Sullivan, M.J., Petty, N.K., Beatson, S.A., 2011. Easyfig: a genome comparison visualizer. *Bioinformatics* 27 (7), 1009–1010. <https://doi.org/10.1093/bioinformatics/btr039>.
- Thompson, F.L., Iida, T., Swings, J., 2004. Biodiversity of vibrios. *Microbiol. Mol. Biol. Rev.* 68 (3), 403–431. <https://doi.org/10.1128/MMBR.68.3.403-431.2004>.
- Thompson, J.D., Higgins, D.G., Gibson, T.J., 1994. CLUSTAL W: improving the sensitivity of progressive multiple sequence alignment through sequence weighting, position-specific gap penalties and weight matrix choice. *Nucleic Acids Res.* 22 (22), 4673–4680. <https://doi.org/10.1093/nar/22.22.4673>.
- Tran, L., Nunan, L., Redman, R.N., Mohney, L.L., Pantoja, C.R., Fitzsimmons, K., Lightner, D.V., 2013. Determination of the infectious nature of the agent of acute hepatopancreatic necrosis syndrome affecting penaeid shrimp. *Dis. Aquat. Org.* 105 (1), 45–55. <https://doi.org/10.3354/dao02621>.
- Turner, D., Kropinski, A.M., Adriaenssens, E.M., 2021. A roadmap for genome-based phage taxonomy. *Viruses* 13 (3), 506. <https://doi.org/10.3390/v13030506>.
- Turner, D., Kropinski, A.M., Alfarnas-Zerbini, P., Buttimer, C., Lavigne, R., Bister, J.R., Tolstoy, I., Morozova, V.V., Babkin, I.V., Kozlova, Y.N., Tikhunov, A.Y., Tikhunova, N.V., Adriaenssens, E.M., 2019. Create one new family (*Autographiviridae*) including nine subfamilies and 132 genera in the order *Caudovirales* 2019.103B Dann2. Turner@uwe.ac.uk. <https://icvtv.global/ICTV/proposals/2019.103B.zip>. Accessed 3 Aug 2021.
- Tynecki, P., Guziński, A., Kazmierczak, J., Jadczyk, M., Dastyk, J., Onisko, A., 2020. PhageAI - bacteriophage life cycle recognition with machine learning and natural language processing. *bioRxiv* 2020.07.11.198606. doi:10.1101/2020.07.11.198606.
- Vinod, M.G., Shivu, M.M., Umesha, K.R., Rajeeva, B.C., Krohne, G., Karunasagar, I., Karunasagar, I., 2006. Isolation of *Vibrio harveyi* bacteriophage with a potential for biocontrol of luminous vibriosis in hatchery environments. *Aquaculture* 255 (1–4), 117–124. <https://doi.org/10.1016/j.aquaculture.2005.12.003>.
- Yang, H., Ma, Y., Wang, Y., Yang, H., Shen, W., Chen, X., 2014. Transcription regulation mechanisms of bacteriophages: recent advances and future prospects. *Bioengineered* 5 (5), 300–304. <https://doi.org/10.4161/bioe.32110>.
- Yang, M., Chen, H., Guo, S., Tan, S., Xie, Z., Zhang, J., Wu, Q., Tan, Z., 2022. Characterization and genome analysis of a novel *Vibrio parahaemolyticus* phage vB_VpP_DE17. *Virus Res.* 307, 198580. <https://doi.org/10.1016/j.virusres.2021.198580>.
- Yang, M., Liang, Y., Huang, S., Zhang, J., Wang, J., Chen, H., Ye, Y., Gao, X., Wu, Q., Tan, Z., 2020. Isolation and characterization of the novel phages vB_VpS_BA3 and vB_VpS_CA8 for lysing *Vibrio parahaemolyticus*. *Front. Microbiol.* 11, 259. <https://doi.org/10.3389/fmicb.2020.00259>.
- Yu, Q., Xie, J., Huang, M., Chen, C., Qian, D., Qin, J.G., Chen, L., Jia, Y., Li, E., 2020. Growth and health responses to a long-term pH stress in pacific white shrimp *Litopenaeus vannamei*. *Aquacult. Rep.* 16, 100280. <https://doi.org/10.1016/j.aqrep.2020.100280>.
- Yuan, Y., Gao, M., 2016. Proteomic analysis of a novel *Bacillus* Jumbo phage revealing glycoside hydrolase as structural component. *Front. Microbiol.* 7, 745. <https://doi.org/10.3389/fmicb.2016.00745>.
- Zhang, L., Orth, K., 2013. Virulence determinants for *Vibrio parahaemolyticus* infection. *Curr. Opin. Microbiol.* 16 (1), 70–77. <https://doi.org/10.1016/j.mib.2013.02.002>.
- Zhou, X., Massol, R.H., Nakamura, F., Chen, X., Gewurz, B.E., Davis, B.M., Lencer, W.I., Waldor, M.K., 2014. Remodeling of the intestinal brush border underlies adhesion and virulence of an enteric pathogen. *MBio* 5 (4). <https://doi.org/10.1128/mBio.01639-14>.